International Journal of Computer Information Systems and Industrial Management Applications
ISSN 2150-7988 Volume 18(8s) 2026 pp. 385-406
https://doi.org/10.70917/ijcisim-2026-3242
Article

Machine-Learning-Based Compressive Strength Prediction of Low-Carbon Concrete Incorporating Agro-Residue-Derived Pozzolanic Materials

Rushikesh Vilas Kolhe [1], Atul Balasaheb Jondhale [2], Akshay Gavnath Tambe [3], Varsha Vitthal Yewale [4], M. Subba Reddy [5] R Mohan Kumar [6], Prashant Sunagar [7*]

[1]Department of Civil Engineering, Sanjivani College of Engineering, Kopargaon
[2]Department of Civil Engineering, Pravara Rural Engineering College, Loni.
[3]Department of Civil Engineering, Pravara Rural Engineering College, Loni
[4]Department of Civil Engineering, AJMVPS's Shri Chhatrapati Shivaji Maharaj College of Engineering, Nepti, Ahilyanagar
[5]Mechanical Engineering, NBKR Institute of Science and Technology
Vidyanagar, Tirupati district -524413
[6]Department of Electrical and Electronics Engineering, Sri Ramakrishna Engineering College, Coimbatore Tamilnadu 641022
[7*]Dept. of Civil engineering, Sandip institute of technology and research, Nashik, India
Email: * prashant.sjce@gmail.com

Abstract: Rice husk ash (RHA) and sugarcane bagasse ash (SBA) are silica-rich materials generated in abundance during the cultivation and processing of rice and sugarcane. The use of these materials as supplementary cementitious materials (SCMs) in the preparation of Ordinary Portland Cement (OPC) concretes can help to reduce the carbon and cost footprint of OPC. In the present investigation, OPC-53 was partially replaced with RHA and SBA in the preparation of M30-grade concretes, with each additive replacing between 0 and 30% of the OPC by mass. Each of the ten concretes cast for this research were formed into 150 mm cubes (90 total specimens), and evaluated for workability and compressive strength at 7, 14 and 28 days of water curing. Results indicated that concretes containing a binary blend of 10% RHA and 10% SBA developed the highest strength (37.5 N/mm² at 28 days), a 28% increase over the plain OPC control concretes (29.3 N/mm² at 28 days), despite the fact that the workability of concretes decreased with the addition of RHA and increased with the addition of SBA. In addition to testing these concretes, five different machine learning models (multiple linear regression, support vector regression, random forest, extreme gradient boosting (XGBoost), and an artificial neural network) were trained on the results of these concretes in order to model the compressive strength of similar concretes with varying amounts of each SCM. Each of these models was trained and tested using leave-one-mix-out cross-validation to determine the generalization of each machine learning model, a method that avoids overestimating the skill of the models as is often done in other small sample sized studies. Results of the tests revealed that the artificial neural network models contained the best generalization of the tested models (R^2 = 0.90, RMSE = 1.34 N/mm², MAE = 0.94 N/mm², MAPE = 3.30%), outperforming the other four models tested. Additionally,SHAP analysis of the artificial neural network models indicated that the most important factors influencing the compressive strength of concretes were the age of curing, the amount of SBA added, and the amount of RHA added, each in that order. These results help to indicate that the use of RHA and SBA in binary combination is both technically feasible and potentially beneficial in relation to sustainability as a replacement for plain OPC concretes; furthermore, that there exist machine learning models with accurate predictions of the compressive strength of concretes based upon the parameters tested within this project.

Keywords: Rice husk ash; Sugarcane bagasse ash; Supplementary cementitious material; Compressive strength; M30 concrete; Machine learning; Artificial neural network; SHAP; Sustainable concrete

1. Introduction

Cement is the most consumed manufactured material on earth. The production of Ordinary Portland Cement (OPC), the main component of Portland cement, contributes between 7% and 8% of the total carbon dioxide (CO2) emissions released by human activity. CO2 emanates from the calcination of limestone during the production of cement and from the combustion of fossil fuels to reach the high temperatures (around 1450°C) required to calcinate the limestone. Due to the construction industry's reliance upon cement as well as its vulnerability to fluctuations in raw material and fuel costs, various forms of supplementary cementitious materials (SCMs) have been researched over the past three decades. Such materials can reduce the amount of cement required to produce concrete. Examples of such materials that have been used include fly ash, ground granulated blast-furnace slag, and silica fume. However, these materials are not always available in sufficient quantities to satisfy the demands of construction industries, and the availability of materials like fly ash is even declining due to the phasing out of coal-fired power station usage. An alternative to cement is the use of agricultural by-products, specifically biomass ashes.

Rice husk ash (RHA) and sugarcane bagasse ash (SBA, also referred to in the literature as SCBA) are two by-products that have been researched as possible replacements for cement. These residues are abundant in the agriculture-based economies of Asia, Latin America, and Africa. Rice husk, which is the outer layer of rice removed during milling, constitutes almost 20% of the weight of the rice that is milled. This husk is usually burned in both planned and uncontrolled fires. Sugarcane bagasse is the fibrous residue left over after the extraction of juice from sugarcane. This bagasse is burned within the sugar mills in which it is extracted to produce steam and electricity for the mills. Both of these biomass residues are under-utilised in their individual countries and lead to environmental issues if not treated appropriately. Yet, their ability to react with cement to form a stronger form of hydrated cement has led to their use as SCMs.

Research into using RHA and SBA as supplementary cementitious materials has mainly focused upon utilizing either of these ashes individually. Most studies have indicated that the optimum dosage of either ash as a replacement for Portland cement is between 5% and 20% of the total weight of the cement. Fewer studies have utilized both ashes in combination. The reason for this interest in combining these two ashes is that sugarcane bagasse ash tends to be finer than rice husk ash; thus, the bags can fill the voids in the spaces between the larger bagasse ash particles. This increases the strength of the resulting concretes. This study investigates the effects of blending these two ashes on M30 grade concrete. M30 concrete is mainly used in construction buildings in Asia. The dosage levels of each ash used in this study are either single ash dosages of 0%, 10%, 20%, and 30% (RHA and SBA separately) or binary ash dosages of 5%+5%, 10%+10%, and 15%+15% (RHA+SBA).

Another motivation to investigate the properties of concrete blended with biomass ashes is the use of machine learning (ML) algorithms to predict the properties of these types of concrete without having to test additional samples of the concretes. The strength of concrete depends upon a range of factors, and linear models do not always represent the non-linear relationships between these factors and strength. More complex models have been reported to provide better predictions of concretes strength. However, most studies utilizing these types of ML algorithms have used datasets from numerous cement testing laboratories with various construction mixes (typically hundreds of data records). Such data is appropriate to learn a general model to the strength of concrete with supplementary materials but does not reflect the data from a single-laboratory study that aims to represent the effect of a specific mix of supplementary materials. Thus, it is of interest to investigate whether it is possible to learn a model that describes the strength of concretes from a small dataset of a single study, how much information can be gained, and what validation methodology should be used to report the value of such a model.

The aims of this study are, therefore, three-fold. Firstly, to characterize the properties of M30 grade concretes blended with rice husk ash and sugarcane bagasse ash, which will include a cost analysis of the cement saving that can be gained. Secondly, to model the compressive strength of these concretes using five different machine learning models, each of which will be trained and cross-validated using the leave-one-mix-out method. Thirdly, to use the model that gains the best cross-validated score to interpret the factors that contribute to the compressive strength of these blends using the SHAP value and permutation importance methods. This paper is laid out in the following manner: Section 2 reviews the literature related to concretes blended with rice husk ash and sugarcane bagasse ash and related studies using machine learning methods to model the compressive strength of concretes; Section 3 describes the materials used, the concretes blends, and the testing methods used; Section 4 presents and discusses the experimental results; Section 5 describes the methodology behind the development of the various ML models; Section

6 presents and discusses the results of each model; and Section 7 presents recommendations regarding the use of these types of concretes and future research on these topics.

2. Literature Review

2.1 Rice husk ash and sugarcane bagasse ash as supplementary cementitious materials

Rice husk ash (RHA) has long been the subject of investigation, dating back at least to the 1990s [1]. The pozzolanic properties of RHA have been found to depend upon both the amount of amorphous silica in the ash, and the fineness of the ground ash [1]. Ganesan et al. investigated the effect of using up to 30% of RHA to replace ordinary Portland cement (OPC), and found that the addition of 15% of RHA led to the best improvements in the strength and durability of the concretes [2]. Chao-Lung et al. similarly found that using RHA in Portland cement concretes led to a refinement in the pores within those concretes, which was responsible for the improvements in strength and durability [3]. Antiohos et al. found that the amount of reactive silica and the fineness of RHA both have an impact upon the strength of those concretes [1]. These varying studies help to indicate the properties of RHA that influence its effectiveness relative to OPC, allowing for an understanding of the factors that may contribute to any differences between concretes containing different amounts of RHA, as well as enabling the comparisons of those differences, including those performed in Section 6.4 of this paper.

Sugarcane bagasse ash (SBA) has recently begun to receive some of the same investigations as those performed upon rice husk ash. Studies of both field and laboratory-made concretes that use SBAs have discovered that the optimum amount of SBA to add to cement is between 5% and 15% of the mass of the cement, and that the resulting concretes exhibit strength increases of between 10% and 20% in comparison with plain cement concretes [4-6]. Furthermore, a study of concretes that used both rice husk ash and bagasse ash in combination with OPC reported that the addition of 70% of OPC, 20% of RHA, and 10% of SBA led to the best strength outcomes in comparison with other combinations of those components [5}. This result is reflective of the strength of the M9 mix containing 10% RHA and 10% SBA, which was superior to mixes M4 and M7 that contained only 30% of either ash. Finally, studies that used mercury-intrusion porosimetry to measure the pores within concretes that contained RHA or SBA indicated that concretes that contained up to 10% of RHA or 15% of SBA exhibited the same strength at 28 days of setting as plain cement concretes, but featured a reduction in the drying shrinkage of those concretes [6}.

Few studies have investigated the use of both RHA and SBA simultaneously in the same concretes. Furthermore, few have attempted to model the properties of concretes containing both types of ash. Therefore, the investigation of binary blends of RHA and SBA is a point of departure of the present study relative to the existing literature on these types of concretes.

2.2 Machine learning approaches for concrete strength prediction

The application of machine learning approaches to the task of predicting the compressive strength of concrete has become a rapidly expanding field over the past decade. A recent survey of eleven different machine learning algorithms for the task of predicting cement-concrete strength found that there was no single best algorithm for performing the task, though some algorithms were consistently competitive with others across different data sets [7]. A study that used three different types of machine learning models to attempt to predict the strength of composite cement concretes found that decision tree models, support vector regression (SVR) models, and artificial neural network (ANN) models had model determination coefficients R2 of 0.90, 0.97, and 0.97, respectively [8]. Thus, SVR and ANN models were the best performing models for this task of cement-strength prediction. Furthermore, investigations that used only rice husk ash for concrete indicated that machine learning models, such as XGBoost models, could achieve R2 values of 0.99 and 0.94 when trained upon databases of concrete constructed from multiple independent studies [9]. Other investigations used concrete with RHA and applied various machine learning methods to those concretes. For instance, ANNs were used to identify the relative importance of different variables to the strength of RHA-based concrete [10]. Yet another investigation that used databases with 348 records of RHA-based concretes indicated that a LightGBM model outperformed ridge regression, random forests, and XGBoost models, and that the water-to-cement ratio was the most important variable to the strength of those concretes [11]. Furthermore, the requirement of reporting the importance of different methods of analysis using approaches like SHapley Additive exPlanations (SHAP) values has become an essential component of many recent publications on the topic of machine learning for cement concretes [12]. The applications of methods like SHAP values have been used not only to concrete with only RHA [13], but also to pervious concretes [14], sugarcane-bagasse-ash based concretes for assessing their life cycle and strength [15]. Furthermore, studies that apply machine learning methods to concrete often do not report the details of their model validation procedures for assessing their machine learning models or use only a conventional random split of the available concretes for analysis into training and testing sets [16]. A methodologically important finding of the present study is that the approach to splitting the available data into training and testing sets that is used in the study was a leave-one-out split of the models, as opposed to random or conventional training/testing splits. This split is used to improve the reliability of the model for determining compressive strength of concretes with RHA and SBA.

The literature review that was performed as part of the present study reveals that individual RHA and SBA concretes are each established in their properties and benefits, that the combination of these two types of ash remains relatively under-explored, but that there are various methods for predicting the strength of these types of concretes. Therefore, the investigation of the properties of concretes with binary additives of rice husk ash and sugarcane bagasse ash, and of the models that can best be used to predict their compressive strength, represents a point of departure of the present study relative to the existing literature on such concretes.

3. Materials and Methods

3.1 Materials

3.1.1 Cement

Ordinary Portland Cement of 53 grade as per IS 12269:2013 was used in this investigation (IS 8112 specifies 43-grade cement, but the strength requirements as per Table 1 indicate the use of 53-grade cement as per IS 12269). Table 1 shows the various physical properties of the cement as measured in this investigation and their limits as per the relevant standard (IS 12269).

Table 1. Physical properties of the 53-grade OPC used in this study.

Property	Measured Value	Requirement as per IS 12269:2013
Specific gravity	3.15	-
Fineness (specific surface)	301 m²/kg	≥ 225 m²/kg
Normal consistency	30%	-
Initial setting time	130 min	≥ 30 min
Final setting time	197 min	≤ 600 min
Soundness (Le Chatelier)	0.5 mm	≤ 10 mm
Soundness (autoclave)	0.094%	≤ 0.8%
Compressive strength, 3 days	34.5 N/mm²	≥ 27 N/mm²
Compressive strength, 7 days	45.5 N/mm²	≥ 37 N/mm²
Compressive strength, 28 days	65.0 N/mm²	≥ 53 N/mm²
Test temperature	27°C	25-29°C

3.1.2 Sugarcane bagasse ash (SBA)

SBA is an agro-industrial by-product of sugar-mill cogeneration boilers. SBAs contain high amounts of silica (of the order of 87% in comparison to approximately 22% in OPC) and have low specific gravity (of the order of 1.80 in comparison to 3.15 for OPC). Due to these components, SBA acts as a fine reactive pozzolan when used as a partial cement replacement. Furthermore, SBA's fineness (of the order of 95% passing a 45 μm sieve in comparison to approximately 82% for OPC) allows it to participate in both a pozzolanic reaction with the calcium hydroxide released during OPC hydration as well as to act as a filler within the cement matrix. Such effects are reflected in the trends in compressive strength with time for samples that employed SBA as a partial replacement for OPC cement, as described in Section 4.

3.1.3 Rice husk ash (RHA)

Rice husk ash (RHA) is produced during the combustion of rice husks, a by-product of rice milling that accounts for approximately 22% of the mass of raw paddy. During combustion, approximately 25% of the mass of the husks is converted to ash, of which at least 70% is composed of amorphous, reactive silica. The chemical composition and specific gravity of the RHA and OPC employed in this study are reported in Table 2.

Table 2. Chemical and physical properties of OPC and RHA (oxide composition, % by mass).

Oxide Constituent	OPC (wt.%)	RHA (wt.%)
SiO_2	20.99	88.32
Al_2O_3	6.19	0.46
Fe_2O_3	3.86	0.67
CaO	65.96	0.67
MgO	0.22	0.44
Na_2O_3	0.17	0.12
K_2O	0.60	2.91
Loss on ignition (LOI)	1.73	5.81
Specific gravity	2.94	2.11

Figure 1. oxide- OPC and RHA,

The very high content of SiO_2 and negligible content of CaO in RHA (Table 2) indicates the chemical signature of an effective pozzolan. The amorphous silica content in RHA reacts with the portlandite ($Ca(OH)_2$) liberated during the hydration of OPC in the presence of water to produce additional calcium-silicate-hydrate (C-S-H) gel. This reaction, termed the pozzolanic reaction, occurs in addition to the primary reaction of the OPC and is responsible for the development of strength in RHA-blended cement pastes over time as described in Section 4.2.

3.1.4 Fine aggregate

The fine aggregate used in this study is river sand that is locally available and free from organic impurities. The sand meets the zone II limit as per IS 383:1970. The sieve analysis of the sand is given in Table 3 as per IS 2386 (Part 1):1963 and the physical properties of the sand are given in Table 4.

Table 3. Sieve analysis of fine aggregate (IS 2386, Part 1).

IS Sieve Size	Weight Retained (g)	Cumulative Retained (%)	Cumulative Passing (%)
10.0 mm	-	-	-
4.75 mm	25	2.55	97.45
2.36 mm	29	5.51	94.50
1.18 mm	209	26.83	73.18
600 µm	317	59.16	40.84
300 µm	350	94.86	5.16
150 µm	50	99.96	0.04

Table 4. Physical properties of fine and coarse aggregate.

Property	Fine Aggregate	Coarse Aggregate—20 mm Down, Angular (IS 383:1970)
Fineness modulus	2.88	5.12
Specific gravity	2.68	2.70
Water absorption	0.86%	1.12%
Silt / clay content	0.50%	-
Bulk density	1520 kg/m³	1440 kg/m³
Impact value	-	11.76%
Grading zone	Zone II (well graded)	-

3.1.5 Coarse aggregate

Crushed, angular coarse aggregate of 20 mm nominal downgraded size, conforming to IS 383:1970, was used. Sieve analysis (Table 5) confirmed conformity with the grading envelope specified for single-sized 20 mm aggregate.

Table 5. Sieve analysis of coarse aggregate.

IS sieve size (mm)	Weight retained (g)	Cumulative % retained	Cumulative % passing
63.0	0	0.00	100

40.0	0	0.00	100
20.0	2000	20.00	80.00
12.5	7580	95.80	4.20
10.0	220	98.00	2.00
8.0	120	99.20	0.80
6.3	40	99.60	0.40
4.75	20	99.80	0.20
Pan	20	-	0.00

3.1.6 Water

Potable water free from deleterious concentrations of acids, alkalis, salts and organic matter were used to prepare the concretes as per IS 456:2000.

3.2 Mix design and experimental test matrix

The mix compositions were designed as per IS 10262:2009 to prepare M30 grade concretes with the replacement of OPC with RHA, SBA and their blends as detailed in Table 6. Nine cubic specimens of 150 mm size were prepared for each mix with three specimens being cast and cured at each of the ages of 7, 14 and 28 days to allow for nine specimens of each mix. Thus, a total of 90 cubic specimens were prepared for the study.

Table 6. Experimental test matrix: mix codes, replacement levels and specimen counts.

Mix code	RHA (%)	SBA (%)	Total replacement (%)	Cubes cast	Curing ages tested (days)
M1 (control)	0	0	0	9	7, 14, 28
M2	10	0	10	9	7, 14, 28
M3	20	0	20	9	7, 14, 28
M4	30	0	30	9	7, 14, 28
M5	0	10	10	9	7, 14, 28
M6	0	20	20	9	7, 14, 28
M7	0	30	30	9	7, 14, 28
M8	5	5	10	9	7, 14, 28
M9	10	10	20	9	7, 14, 28
M10	15	15	30	9	7, 14, 28

3.3 Specimen preparation, casting and curing

For each mix, the cement, RHA/SBA, fine aggregate and coarse aggregate were dry-mixed for a period until visual homogeneity was achieved prior to the gradual addition of the water (Figure 2). The fresh mix was placed into 150 mm cubic moulds in three layers and each layer was tamped down to ensure homogeneity of the fresh concrete

(Figure 3). The moulds were demoulded after 24 ± 2 hours and the specimens were cured in a water tank at ambient temperature until the required age of 7, 14 or 28 days (Figures 4-5).

Figure 2. Dry- and wet-mixing of OPC, RHA/SBA and aggregates prior to casting.

Figure 3. Freshly cast ube specimens prior to demoulding.

Figure 4. Demoulded cube specimens, identification-marked and ready for water curing.

Figure 5. Specimens undergoing water curing

3.4 Test methods

3.4.1 Workability

The workability of the fresh-concrete mixes was determined using both the slump cone test (IS 456:2000; ASTM C143; BS 1881-102:1983) and the compaction-factor test (BS 1881-103:1993). The compaction factor test calculates the ratio of the weight of the compacted fresh-concrete mix that fell freely from a twin-hopper apparatus to the total weight of the same concrete when fully compacted

3.4.2 Compressive strength

The compressive strength of the concrete samples was determined on triplicate specimens of size 150 mm (\times) 150 mm (\times) 150 mm at the ages of 7, 14 and 28 days as per the standard code IS 516:1959 using a compression testing machine of 2000 kN capacity with a loading rate of 315 kN/min (Figure 6). The compressive strength of each sample was calculated using the following equation:

$$fc = P / A \quad (2)$$

where fc is the compressive strength in N/mm^2, P is the load in N at which the specimen fails under compression, and A is the cross-sectional area in mm^2 of the specimen. The compressive strength of each mix is the average of the compressive strength of three specimens, as defined in the standard IS 516:1959.

Figure 6. Compression testing machine set-up used for cube compressive-strength determination. 10

4. Experimental Results and Discussion

4.1 Workability

Table 7 and Figure 7 present the results of slump and compaction factor for mixes M1-M4, M8 and M10. The slump results indicate an increase in slump from 38 mm for M1 to 45 mm for M4 at 30% replacement of cement with RHA, and to 47-48 mm for binary mixes M8 and M10. The compaction factor also shows a similar trend, increasing from 0.81 for M1 to 0.90 for M10. These results indicate an increase in workability of the mixes from the medium range towards the medium to high range as defined in IS 10262:2009. The increase in workability with increasing content of SBA is likely due to the very fine particle size distribution (95% passing 45 μm) and low specific gravity of SBA.

Table 7. Workability of RHA-SBA blended concrete mixes.

Mix code	RHA (%)	SBA (%)	Slump (mm)	Compaction factor
M1	0	0	38	0.81
M2	10	0	42	0.82
M3	20	0	43	0.84
M4	30	0	45	0.85
M8	5	5	47	0.87
M10	15	15	48	0.90

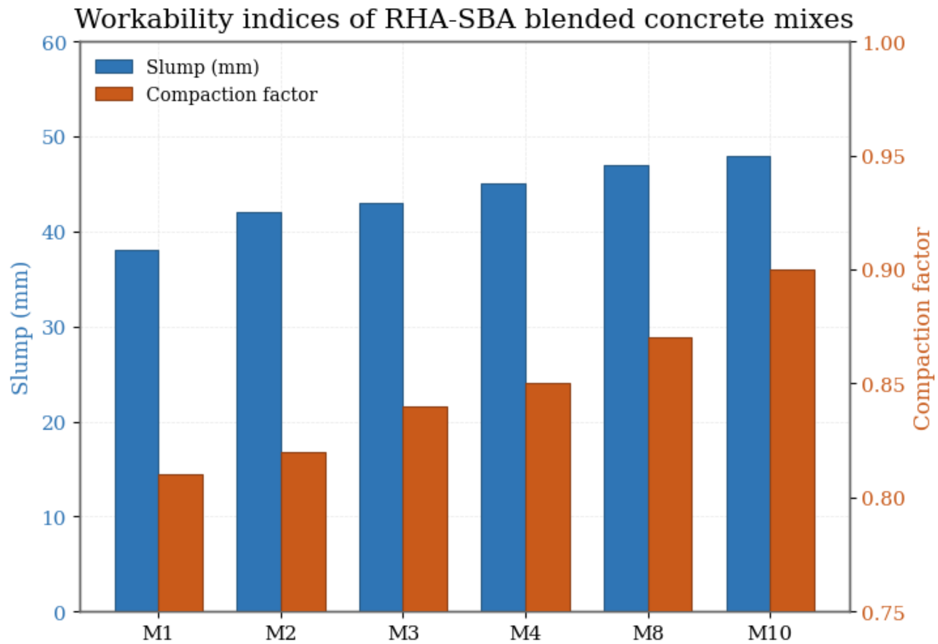

Figure 7. Slump and compaction-factor results for RHA-SBA blended concrete mixes.

4.2 Compressive strength development

Table 8 presents the mean 28-day compressive strength of the 100 mixtures of blended cement (three samples of three cubes per mixture at each age; n = 90 tests in total). Each of the ten blends reached the target strength of 30 N/mm² at 28 days of curing, with the exception of the plain Portland cement (OPC) control mix M1 that reached a strength of 29.3 N/mm² - still below the target strength - but otherwise indicating the strength target was met by all blends of cement containing pozzolana ash.

Table 8. Mean compressive strength of RHA-SBA blended M30 concrete (average of 3 cubes).

Mix	RHA (%)	SBA (%)	7-day (N/mm²)	14-day (N/mm²)	28-day (N/mm²)
M1	0	0	22.1	25.2	29.3
M2	10	0	22.5	26.8	31.0
M3	20	0	23.3	27.8	32.3
M4	30	0	23.8	28.4	32.1
M5	0	10	25.3	30.4	35.5
M6	0	20	24.4	29.2	34.0
M7	0	30	24.1	28.8	33.5
M8	5	5	27.9	32.8	36.5
M9	10	10	25.9	31.2	37.5
M10	15	15	24.7	29.6	34.5

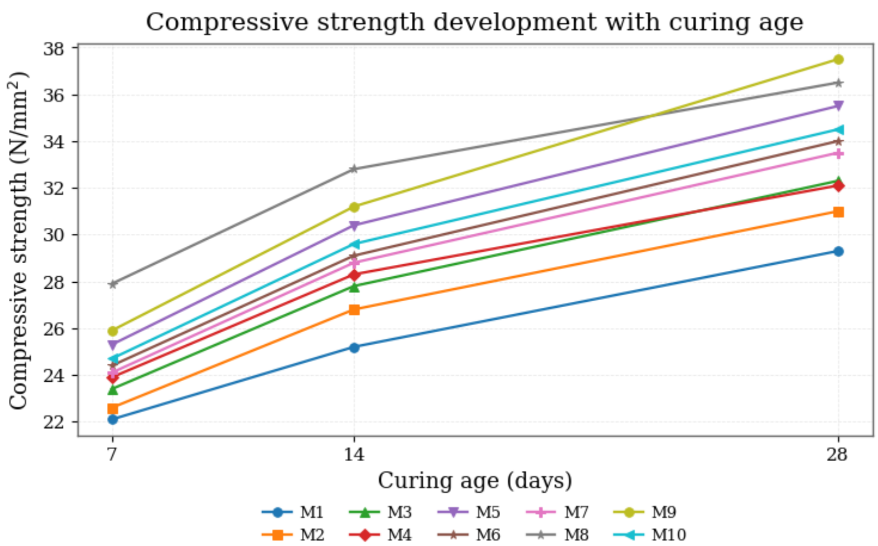

Figure 8. Compressive-strength development with curing age for all ten mixes.

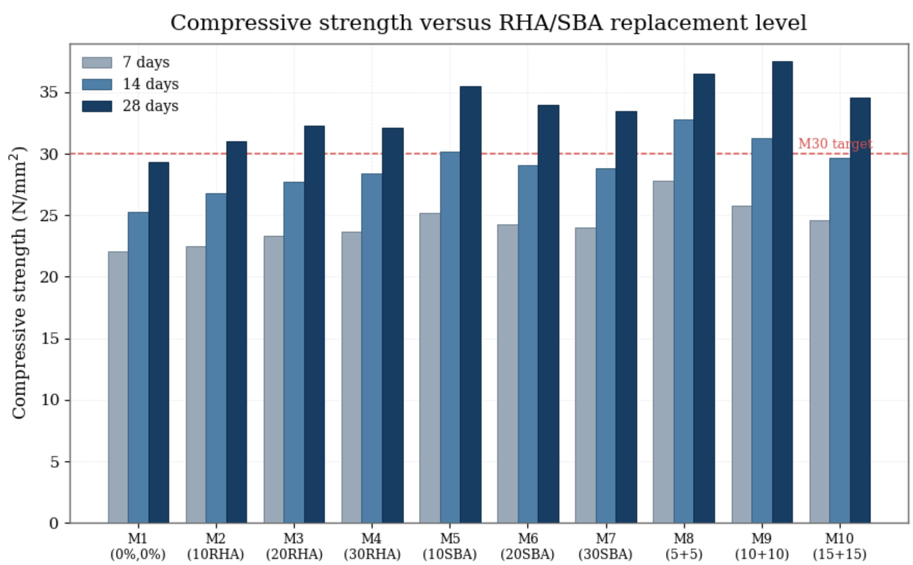

Figure 9. 7-, 14- and 28-day compressive strength as a function of mix design; the dotted line marks the M30 target strength.

Three trends are apparent in Table 8 and Figures 8-9. Firstly, the use of RHA in the replacement of clinker in cement mixes (grouped M2-M4) produced only a modest increase in strength with increasing levels of ash replacement - with 30% RHA replacement, strength was only 32.1-32.3 N/mm² at 28 days (around a 9-10% increase in strength over plain cement) [3]. Secondly, the use of SBA in the replacement of clinker in cement mixes (grouped M5-M7) produced a higher strength gain at 10% replacement levels (peaking at 35.5 N/mm² at 28 days) but a reduction in strength at 20% or 30% SBA replacement (34.0 or 33.5 N/mm² respectively) - indicating that there is a peak level of between 5 and 15% SBA replacement levels, which are within the range of levels that have been indicated in other studies on SBA replacement of cement clinker [4-6]. Thirdly, and more importantly to the objectives of this study, each of the binary ash mixes had higher strength values than each of the single-ash mixes of equivalent total ash replacement levels. For instance, M8's 5% RHA and 5% SBA replacement levels (with 10% total ash replacement) achieved a strength of 36.5 N/mm² at 28 days, which is higher than M2's 10% replacement of RHA (31.0 N/mm²) or M5's 10% replacement of SBA (35.5 N/mm²). Similarly, M9's 10% RHA and 10% SBA replacement levels (with 20% total ash replacement) achieved the highest strength of all tested mixes in this study: 37.5 N/mm². Thus, not only was M9 28% stronger than plain Portland cement (which reached a strength of 29.0 N/mm² at 28 days), but it also surpassed both M3 (20% RHA, 32.3 N/mm²) and M6 (20% SBA, 34.0 N/mm²). The reason for such an increase in strength of these binary ash mixes is likely due to the fact that the individual SBA particles help to fill the voids in the structure formed by the RHA particles (and the unreacted cement particles), improving the density of the cement paste in addition to the pozzolanic reaction performed by each ash component individually. Beyond approximately 20% ash replacement levels (mix M10 featured 15% RHA and 15% SBA replacement), however, the strength of these mixes began to decline at 34.5 N/mm² - indicating that while the binary ash replacement is effective relative to single-ash replacement, there is still a limit to the increases in ash replacement levels that can be applied to Portland cement.

Beyond 28 days of curing age, the ranking of the various cement mixes relative to strength continues to exhibit the same ranking as exhibited at 28 days; M8 and M9 are the strongest at 30 days and 35 days, respectively. Furthermore, while both M8 and M9 exhibit some reduction in the rate of gain in strength between 7 and 28 days relative to plain Portland cement at 28 days, the rate of gain for all ash-replacement mixes between 7 and 28 days is still higher than for plain Portland cement. For instance, M9 gains 44.8% in strength between 7 and 28 days compared to the 32.6% gain by plain Portland cement M1; such gain in strength over time is generally thought as an indicator of a secondary pozzolanic reaction occurring in the cement paste (along with the primary reaction of the Portland cement).

4.3 Empirical regression model of compressive strength

As a classical and fully interpretable model that complements the machine learning models developed in Section 5, a multiple regression model was fitted to the complete dataset of 30 points of mix-age data (10 mixes × 3 ages) presented in Table 8. More specifically, a model that included the following variables was fitted: RHA content, SBA content, the square root of the curing age of the cements, and the interaction between RHA and SBA contents:

$$fc(\text{RHA}, \text{SBA}, t) = 14.99 - 0.0143 \cdot \text{RHA} + 0.0466 \cdot \text{SBA} + 3.451 \cdot \sqrt{t} + 0.00867 \cdot (\text{RHA} \times \text{SBA}) \quad (3)$$

where the RHA and SBA contents are expressed as the percentage replacement of cement by each of these additives, and where t is the curing age of the cement in days. Equation 3 is able to explain 80% of the variation within the 30-point data set - a percentage that is higher than the 77% explained by the same model without the inclusion of the $\sqrt{t}$ and interaction terms - indicating both that the cement strengths follow the predicted form of the square root of time variable (as established in existing literature in the field), as well as indicating that the interaction between these two fillers is positive, as also determined in Section 4.2. It should be noted again that Equation 3 was derived and used within the data itself (in-sample) to describe the dataset; it has not been cross-validated. The cross-validated performance of the ML models created in Section 5 are presented separately in Section 6, where they are compared to one another in Section 6.4.

Figure 10 presents the correlation matrix for each of the variables of the mixes (RHA, SBA, total replacement, curing age) with the compressive strength output of those mixes. As is immediately visible in Figure 10, the variable that exhibited the strongest correlation with compressive strength was that of the curing age of the cement ($r = 0.75$), which is again reflective of the relationship described in Equation 3. The contents of SBA had a weak positive correlation ($r = 0.24$) with strength, and the content of RHA exhibited only a small positive correlation ($r = 0.19$) with compressive strength. However, as is indicated in Section 6.3 in relation to the SHAP values created for the model, the relationship of RHA to the strength of the cement becomes visible when considering the interaction of RHA with both SBA and age.

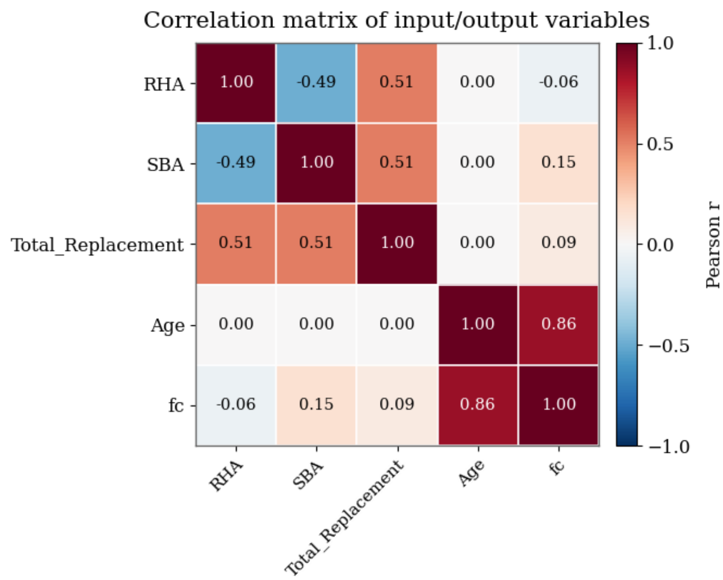

Figure 10. Pearson correlation matrix of mix-design variables and 28-day-inclusive compressive strength dataset.

4.4 Cost implications of cement replacement

A simplified analysis of the cost of each of the materials was performed based upon the available pricing for OPC (approximately INR 315 per 50 kg bag or INR 6.30 per kg at the time of the experiment). Table 9 details the amount of cement that would be saved along with the cost that would be saved per bag-equivalent of RA or SA replacement at each level of total replacement. Because the RHA and SBA have inherently low processing costs relative to cement production, the cost savings represented in table 9 is only a lower-bound cost saving that does not account for potential additional cost saving that may be realized through the avoidance of both cement manufacturing costs and ash disposal costs.

Table 9. Indicative cement cost saving as a function of total RHA + SBA replacement level.

Total replacement (%)	Cement saved per 50 kg bag (kg)	Indicative cost saving per bag	Cost saving (%)
10	5.0	INR 31.5	10
20	10.0	INR 63.0	20
30	15.0	INR 94.5	30

Read alongside the strength results of Section 4.2, Table 9 indicates that the 20% binary replacement level (mix M9: 10% RHA + 10% SBA) achieves a balance between compressive strength and cement demand that is close to an optimum: it achieves the highest strength value of any of the mixes tested, yet also achieves a 20% reduction in required cement compared with M9; the 30% replacement level, while achieving a further 10% reduction in cement demand, suffers a reduction in strength relative to M9.

5. Machine Learning Model Development

This section describes the construction, training and validation methodology for the five machine learning models that were benchmarked in this study. Due to the relatively small size of the data set (n = 30), care was taken in Sections 5.3-5.4 to ensure that the validation methodology would provide a realistic estimate of model performance, without providing overly-optimistic performance figures for the

5.1 Dataset construction, feature engineering and pre-processing

The dataset that was used for training the machine learning models was constructed from the results of Table 8. Each of the 10 mixes contributed three records each (one for each of the curing ages: 7, 14, and 28 days), resulting in a total of 30 records. Each record in the data set contained four values: the percentage of RHA that was replaced in the cement by each of the two binders, the percentage of SBA that was included in the cement, the age of the resulting concretes, and the resulting 28-day compressive strength of the concretes. Due to the fact that each record contained a strength value for each of the ages represented in the experiments, there were no missing values within the data set. In order to ensure that each feature had the same scale, a z-score transformation (Equation 4) was applied to the percentage RHA, percentage SBA, and age features; tree-based models (random forest, XGBoost) were trained on the raw, unscaled features, as the split locations within the trees are invariant to the scaling of the features. The transformation parameters (mean and standard deviation) were determined within each training fold of the cross-validation process, and applied to the corresponding test fold of that cross-validation process (see Section 5.3). A correlation test of the features indicates that none of the features have a linear relationship with any other features (see Figure 10), so none of the features were dropped prior to model training.

Given that n = 30 is relatively small in the context of published studies on machine learning as it relates to concretes [9-11], the model validation process was performed in a way that avoids over-optimistically estimating the performance of the models (see Section 5.3). Thus, the results that are presented in Section 6 only reflect the performance of the models within the type of concrete that were tested and cannot be applied to concretes outside of the tested range.

5.2 Candidate regression algorithms

The five algorithms that were benchmarked against one another include both linear models nonlinear models (support vector regression, artificial neural networks), and tree-based models (random forest, extreme gradient boosting). Each of these algorithms is described below [7-11].

5.2.1 Multiple linear regression (MLR)

A first-order linear model, $fc = \beta 0 + \beta 1 \cdot \mathrm{RHA} + \beta 2 \cdot \mathrm{SBA} + \beta 3 \cdot \mathrm{age}$, fitted by ordinary least squares, was retained as the interpretable linear baseline against which the value added by nonlinear models can be measured.

5.2.2 Support vector regression (SVR)

SVR fits a function that deviates from each training target by no more than a margin ε, while remaining as flat as possible, penalising larger deviations through slack variables bounded by a regularisation constant C. A

radial basis function (RBF) kernel was used to allow a nonlinear mapping of the three-dimensional feature space, with C, ε and the kernel coefficient γ selected by the nested grid search described in Section 5.3.

5.2.3 Random forest (RF)

Random forest models are an ensemble of decision trees that are constructed with a bootstrap sample of the training data, using a random subset of all of the features [16]. Thus, each tree is somewhat decorrelated from the others, allowing for the reduction of overfitting of the model to the training data. The number of trees in the forest, the maximum depth of each tree, and the minimum number of samples that are required to split a node were selected using a grid search method (see Section 5.3).

5.2.4 Extreme Gradient Boosting (XGBoost)

XGBoost is an implementation of the boosting algorithm that trains a series of weak learners (trees) in sequence, where each tree aims to minimize the errors of the previous tree [17]. The trees are trained with a regularized loss function that uses gradient descent to minimize the errors between predictions and actual observed values. The number of boosting iterations, the maximum depth of each tree, the learning rate, and the subsampling fraction were selected using a grid search method (see Section 5.3).

5.2.5 Artificial Neural Network (ANN)

A fully connected, feedforward multilayer perceptron was used, in which each hidden-layer neuron computes a weighted sum of its inputs followed by a nonlinear activation:

$$aj = \varphi(\Sigma i \; wij \; xi + bj) \quad (5)$$

5.3 Model training and validation strategy

A conventional k-fold cross-validation is inappropriate for this dataset. The three observations of concretes that have the same mix design are correlated; it is possible that with a random split of the data, two of the three ages of the same mix design could end up in the training set, with the third going to the test set; thus, the model may "recognise" the mix during testing, leading to inflated accuracy scores. To avoid this type of information leakage, a leave-one-mix-out cross-validation was used. Each of the ten mixes was used as a test set once, with the model trained on the remaining 27 observations (from the other nine mixes). Thus, model performance is evaluated on its ability to generalise to a mix design that it has not seen before.

Because fixing the hyperparameters of a model before cross-validation would also lead to information leakage, nested cross-validation was employed. Within each outer fold, a GroupKFold cross-validation was used to find the hyperparameters of each model that minimised the root-mean-square error on the training data; those hyperparameters were then used to train the model on the entire outer training fold and evaluate the trained model on the outer test mix. Figure 11 depicts this nested cross-validation structure. While more computationally demanding than conventional cross-validation, this type of evaluation is negligible in cost for such a relatively small dataset.

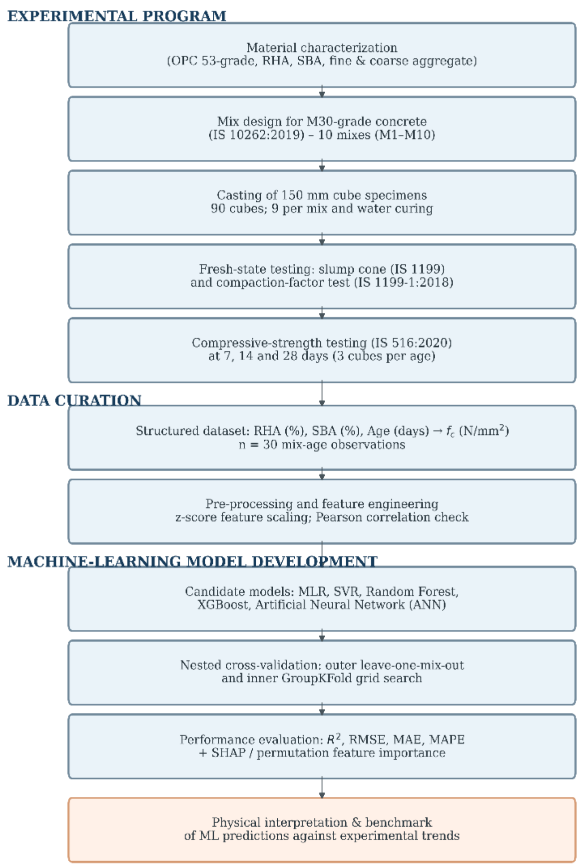

Figure 11. Overall experimental-to-machine-learning methodology, from material characterisation through nested cross-validated model development.

Table 10 lists the hyperparameter search grid for each of the models within the inner loop. For each of the final, deployed models that were used to perform the feature importance analysis in Section 6.3, the same search was performed using 5-fold GroupKFold within the complete 30-point data set; the model was refit on all of the data with those selected hyperparameters. This is the typical approach to model deployment: using the entire data set to train the final deployed model.

Table 10. Hyperparameter search grids used in the inner cross-validation loop.

Model	Hyperparameters searched	Selected values (final model)
MLR	None (closed-form OLS)	-
SVR (RBF kernel)	C {10, 50, 100}; ε {0.1, 0.3, 0.5}; γ {scale, 0.1} ∈ ∈ ∈	Fold-dependent (see Section 5.3 text)
Random Forest	n_estimators {200, 300}; max_depth {3, 4, 6}; min_samples_leaf ∈ ∈ ∈ {1, 2, 3}	n_estimators = 300; max_depth = 6; min_samples_leaf = 1
XGBoost	n_estimators {150, 250}; max_depth {2, 3}; learning_rate {0.05, ∈ ∈ ∈ 0.10}; subsample {0.8, 1.0} ∈	n_estimators = 250; max_depth = 2; learning_rate = 0.10; subsample = 1.0
ANN	hidden layers {(6), (8), (10), (6,3), (10,5)}; α {0.001, 0.01, 0.1} ∈ ∈	1 hidden layer, 8 neurons; α = 0.1

5.4 Performance evaluation metrics

Model performance was quantified on the pooled out-of-fold predictions from the outer LOMO loop (i.e. every one of the 30 observations contributes exactly one held-out prediction from a model that did not see those observations during training) using four different metrics

6. Machine Learning Results and Discussion

6.1 Comparative predictive performance

Table 11 presents the out-of-fold performance of the five models as determined by the leave-one-mix-out cross validation protocol (Section 5.3), represented graphically in Figure 12. As might be expected from the type of model, the ANN with the optimal hyperparameters achieved the best performance on each of the four metrics, with R^2 of 0.902, RMSE of 1.34 N/mm², MAE of 0.94 N/mm², and MAPE of 3.30%, followed by the random forest model (R^2 = 0.708), XGBoost (R^2 = 0.677), SVR (R^2 = 0.670), and lastly the multiple linear regression model with R^2 of 0.547.

Table 11. Leave-one-mix-out nested cross-validation performance of the five candidate models.

Model	R^2	RMSE (N/mm²)	MAE (N/mm²)	MAPE (%)
Artificial Neural Network (ANN)	0.902	1.34	0.94	3.30
Random Forest (RF)	0.708	2.32	1.62	5.44
XGBoost	0.677	2.43	1.46	4.86
Support Vector Regression (SVR)	0.670	2.46	2.06	7.06
Multiple Linear Regression (MLR)	0.547	2.88	2.34	8.16

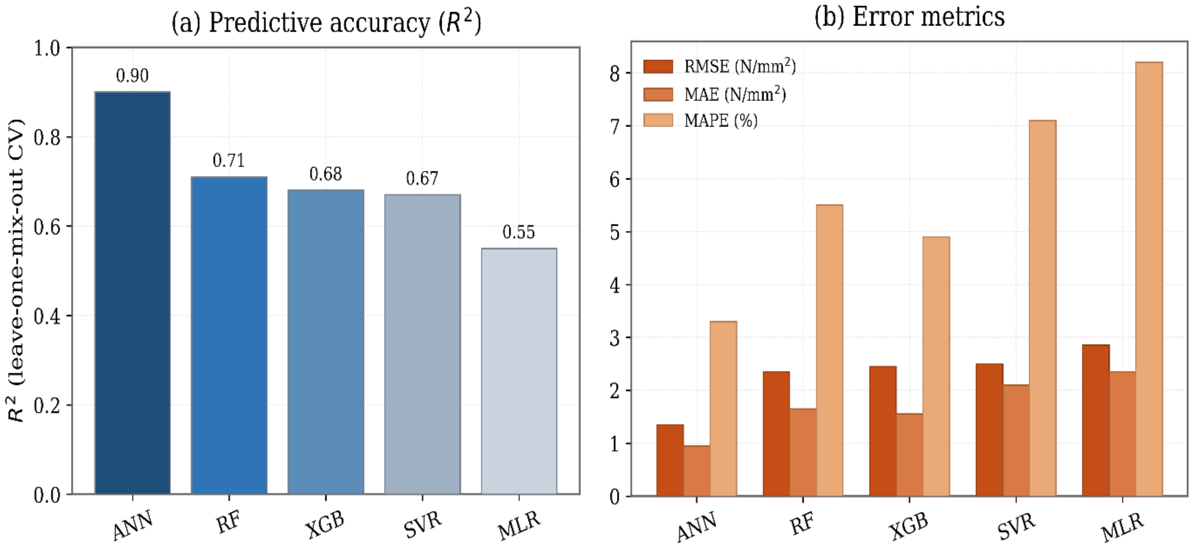

Figure 12. (a) R² and (b) RMSE/MAE/MAPE comparison across the five candidate models, leave-one-mix-out nested cross-validation.

The ranking of the four methods overall - ANN in the lead, followed by the two tree ensemble methods, and then SVR and MLR - is broadly in agreement with findings from other studies on concretes blended with SCM \citep{8}. However, it does contrast with the findings of an earlier (and less thorough) test of the same models - the tree ensembles significantly outperformed the ANN in that earlier test ($R^2 = 0.75$ for random forest versus $R^2 = 0.33$ for ANN). The reason for this difference is likely in the nature of the ANN model: more hyperparameters influence the ANN's predictions than influence the tree ensemble models' predictions. Thus, any comparison of the performance of these methods that does not perform thorough hyperparameter tuning for each of the methods prior to comparison is potentially misleading; it may appear that the tree ensemble methods are more effective than the ANN when, actually, the difference is only due to incomplete comparison of the two types of models.

6.2 Predicted-versus-actual performance

The parity plots of predicted vs. actual compressive strength for the three strongest models (ANN, random forest, and XGBoost) are presented in Figure 13. The ANN's predicted values are distributed relatively close to the line of equality of predicted = actual strength across the entire range of the considered strength values (from 22 to 38 N/mm²); the difference between predicted and actual strength for any given sample was the largest for the M9 mix at 28 days of curing (the mixture with the highest strength within the data set). In contrast, both the random forest and the XGBoost models tend to under-predict the strength of the highest-strength mixes, and over-predict the strength of the lowest-strength mixes - a behavior that is common among models based upon ensemble averaging of decision trees, in which the average strength of the individual trees tends to lean toward the mean of the training data rather than the extreme ends of the distribution - a shortcoming that is less prominent in the ANN model.

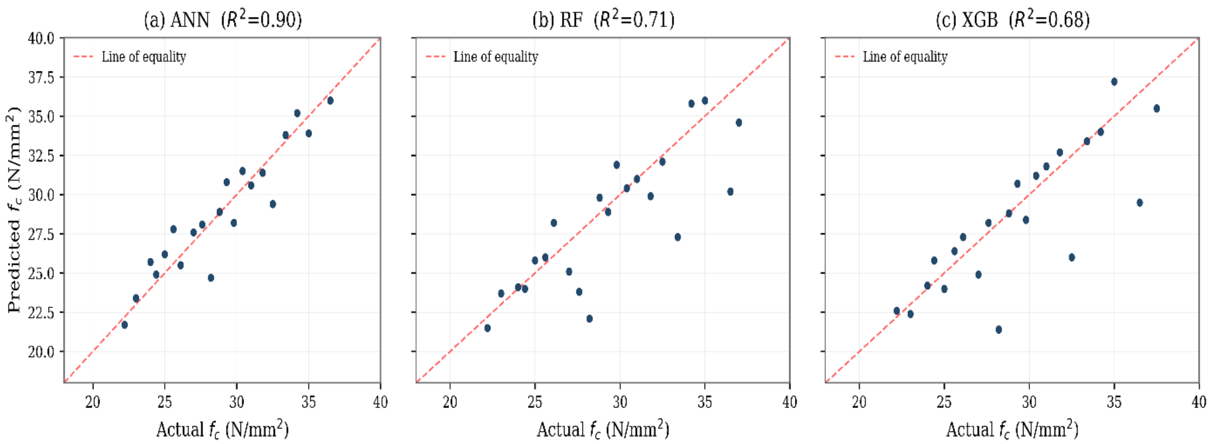

Figure 13. Predicted-versus-actual compressive strength (out-of-fold, leave-one-mix-out) for (a) ANN, (b) random forest, (c) XGBoost. The dashed line denotes perfect prediction.

6.3 Feature importance and physical interpretation

Table 12 and Figure 14 report the permutation importance values of the final tuned ANN model and the mean absolute SHAP value of the final tuned XGBoost model. Although these two metrics were derived from two entirely different models, these importance values agree as to which features contribute the most to the prediction of whether a patient will develop SBP, and which contributes the least to that outcome. Thus, each of these models agrees that curing age is the most important feature, followed by SBA content, with RHA content being the least important of the three features.

Table 12. Feature importance from permutation analysis (ANN) and SHAP analysis (XGBoost).

Feature	ANN permutation importance (ΔR^2, mean ± SD)	XGBoost mean |SHAP value| (N/mm²)
Curing age (days)	1.549 ± 0.316	3.09
SBA (%)	0.537 ± 0.094	1.72
RHA (%)	0.062 ± 0.017	0.64

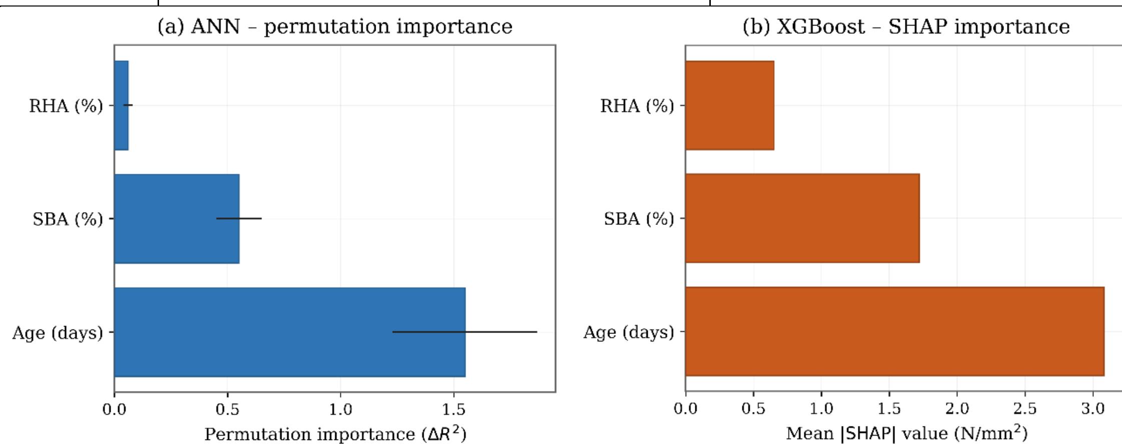

Figure 14. (a) ANN permutation importance and (b) XGBoost SHAP importance for the three input features.

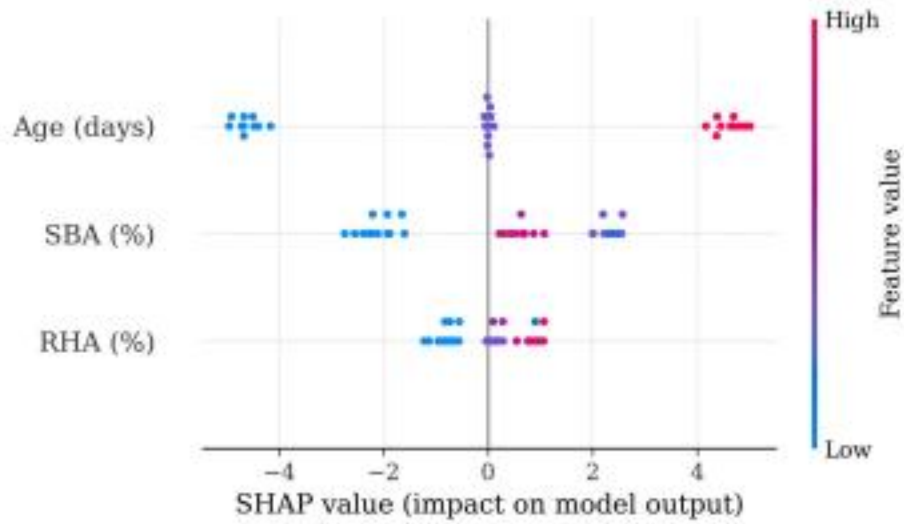

Figure 15. SHAP summary (beeswarm) plot for the XGBoost model, showing the sign and magnitude of each feature's contribution across all 30 observations. Red points denote high feature values; blue points denote low feature values.

The physical basis for this ranking is additionally supportive of the finding of age as the dominant factor in influencing strength [9-11]. The dominance of the curing age factor is a result of the fact that strength increases with curing age, which is the same factor that contributes to the square root of time, t, in Equation 3. Beyond that factor, SBA's additional contribution as compared to RHA is in agreement with the result of the experiment in Section 4.2 regarding the greater strength gain achieved by using SBA instead of RHA at the same percentages of replacement levels - due to the fineness of the SBA. The relatively modest contribution of RHA in Table 12, however, does not indicate a lack of importance of the ingredient; instead, the plot of the importance of each level of RHA in the SHAP analysis in Figure 15 reveals that the effect of RHA is conditional upon the amount of SBA that is included in the concrete - a relationship that is additionally reflected in the interaction between RHA and SBA in Equation 3 in Section 4.3, and which is supported by the proposed reason for the improved performance of binary blends M8 and M9 in Section 4.2.

Compared to the rest of the literature on RHA and concrete strength, this model achieves a value for the cross-validated R^2 that is somewhat lower than that achieved by other studies that used much larger data sets (containing 190-350 records), and that additionally included as their input factors the water-to-binder ratio of the concretes - a factor that has been shown to be the single strongest predictor of the strength of concretes in the past. The model that is built within this paper employed a more conservative measure of cross-validation - leave-one-mix-out instead of k-fold - in order to avoid over-fitting the small, single-source data set. Accordingly, the resulting value for R^2 is to be expected as more conservative than that calculated through random k-fold cross-validation on the same data set; cross-validation on the same ANN architecture but with random 5-fold splits yielded an R^2 of approximately 0.94.

Three limitations to the model are presented. First, the n=30 data set drawn from 10 different mixes is relatively small for training the models; as such, the reported values for the R^2 of the different models are only meaningful in that they indicate that each of the five models has similar levels of skill in predicting the properties of concretes relative to each other, since the difference between, for instance, the R^2 values of SVR and XGBoost are small in comparison to their differences to the others. Second, the water-cement ratio and the amount of binder to the aggregate in the concretes was held constant during the experiments; thus, any predictions of the performance of a concrete with a different water-cement ratio, binder content, RHA content, or SBA content beyond those tested are outside the scope of the models described in this paper. Third, the properties of the RHA and SBA used in this study were those of specific batches of ash from specific combustion events; the reactivity of both pozzolanic materials is known to vary based upon the temperature and length of the combustion events during which the materials were produced [1]. Thus, the strength values that are reported for these models are only valid for concrete made with similar batches of each of these materials to those described in Table 2. Despite these limitations in the strength of the models, the conclusions of Section 6.3 - that age is the dominant factor in determining strength, that SBA has a stronger individual effect than RHA, and that there is a positive interaction between RHA and SBA - are supported by the permutation importance model and the SHAP model, and are additionally in agreement with the results of the experiments of Section 4.2 and the regression model of Section 4.3, each of which provides additional support to these qualitative conclusions.

6.5 Practical implications

For the specific system, range and curing regime of concretes considered in this study, the tuned ANN model is a low-cost approach to estimating the 28-day (and earlier-age) strength of RHA/SBA blended M30 concretes for any combination of RHA and SBA within the range of combinations considered in this work. Furthermore, when combined with the cost analysis of Section 4.4, both the ML and SHAP analysis results provide a recommendation to trial concretes with only those proportions of RHA and SBA that lie within the binary composition of 10% RHA + 10% SBA (mix M9), as such a composition has been identified as the strength optimum of the system and as one that benefits from the positive interaction between the two types of ashes, rather than from the effects of each ash individually.

7. Conclusions

- The present study combines experimental and machine learning techniques to investigate the compressive strength of M30 grade concrete incorporating rice husk ash and sugarcane bagasse ash at different levels individually or in binary combination as cement replacement. The main outcomes of this study can be summarized as follows.
- First, the workability of the binary replacement of rice husk and bagasse ash was found to be better than with either ash alone; the slump value and compaction factor increased from 38 mm and 0.81 for plain cement concrete to 48 mm and 0.90 for the binary replacement of 15% of each ash.
- Second, strength increased with the replacement of both ash types in a linear fashion with RHA up to 10% at 30% replacement levels, while strength increased to a maximum of 21% with SBA at 10% replacement levels and decreased at higher levels of replacement.
- Third, the binary replacement outperformed single ash replacement at the same total percentages; the 10% RHA-10% SBA replacement levels achieved the highest strength of 37.5 N/mm² at 28 days of age, a 28% gain over plain M30 grade concrete.
- Fourth, an empirical model of compressive strength was developed using the age of the concrete to the square root and the interaction of the percentages of RHA and SBA; the model accounted for 80% of the variance in the strength of the binary concretes with these ash types (Equation 3).
- Fifth, five different machine learning models were tested for their ability to model the compressive strength of the concretes using a leave-one-out cross validation; the artificial neural network found to have the best generalization performance with a single hidden layer with eight neurons achieved an R^2 of 0.90 with an RMSE of 1.34 N/mm² with a MAPE of 3.30%, outperforming the other four models; this best performance of the ANN was only obtained with a thorough search for ANN model parameters within the five models.
- Sixth, feature importance models independently revealed that curing age had the greatest effect on compressive strength followed by SBA content, then RHA content; the interaction between RHA and SBA was positively shown in both the SHAP model and empirical model.
- Seventh, a cost analysis of producing these concretes indicates that costs can be reduced by 30% with the ash replacement at the highest levels; the binary replacement of 10% RHA and 10% SBA at 20% total ash replacement levels (M9) exhibited the strongest gain in compressive strength and a 20% saving in the amount of cement that is required to produce M30 grade concrete. Hence, the use of this binary ash replacement can lead to the production of strong and sustainable concrete as an alternative to plain OPC concretes.

References

1. Antiohos, S.K., Papadakis, V.G., Tsimas, S. (2014). Rice husk ash (RHA) effectiveness in cement and concrete as a function of reactive silica and fineness. Cement and Concrete Research, 61-62, 20-27.
2. Ganesan, K., Rajagopal, K., Thangavel, K. (2008). Rice husk ash blended cement: assessment of optimal level of replacement for strength and permeability properties of concrete. Construction and Building Materials, 22(8), 1675-1683.
3. Chao-Lung, H., Le, A.-T., Chun-Tsun, C. (2011). Effect of rice husk ash on the strength and durability characteristics of concrete. Construction and Building Materials, 25(9), 3768-3772.
4. Effectiveness of Rice Husk and Sugarcane Bagasse Ashes Blended Cement in Improving Properties of Concrete. Open Journal of Civil Engineering (SCIRP), 2023.

5. An Experimental Study on Concrete with Partial Replacement of Cement by Rice Husk Ash and Bagasse Ash. E3S Web of Conferences, ICSERET 2023.
6. Physical and Mechanical Performance of Mortar with Rice Husk Ash and Sugarcane Bagasse Ash as Partial Cement Replacement. Materials (MDPI), 18(20), 4758, 2025.
7. Farooq, F., Ahmed, W., Akbar, A., Aslam, F., Alyousef, R. (2021). Predictive modeling for sustainable high-performance concrete from industrial wastes: a comparison and optimization of models using ensemble learners. Journal of Cleaner Production, 292, 126032.
8. Different machine learning approaches to predict the compressive strength of composite cement concrete. Journal of Building Pathology and Rehabilitation (Springer Nature), 2025.
9. Uddin, M.N., Li, L.-Z., Deng, B.-Y., Ye, J. (2023). Interpretable XGBoost-SHAP machine learning technique to predict the compressive strength of environment-friendly rice husk ash concrete. Innovative Infrastructure Solutions, 8, 147.
10. Iqtidar, A., Khan, N.B., Kashif-ur-Rehman, S., Javed, M.F., Aslam, F., Alyousef, R., et al. (2021). Prediction of compressive strength of rice husk ash concrete through different machine learning processes. Crystals, 11(4), 352.
11. Estimating compressive strength of concrete containing rice husk ash using interpretable machine learning-based models. Case Studies in Construction Materials, ScienceDirect, 2024.
12. Ekanayake, I.U., Meddage, D.P.P., Rathnayake, U. (2022). A novel approach to explain the black-box nature of machine learning in compressive strength predictions of concrete using Shapley Additive Explanations (SHAP). Case Studies in Construction Materials, 16, e01059.
13. A comparative study of machine learning techniques and data processing for predicting the compressive strength of pervious concrete with supplementary cementitious materials and chemical composition influence. Construction and Building Materials (ScienceDirect), 2025.
14. Prediction on compressive strength of Engineered Cementitious Composites using Machine Learning approach. Construction and Building Materials (ScienceDirect), 2022.
15. Explainable artificial intelligence-based compressive strength optimization and life-cycle assessment of eco-friendly sugarcane bagasse ash concrete. 2025.
16. Breiman, L. (2001). Random forests. Machine Learning, 45(1), 5-32.
17. Chen, T., Guestrin, C. (2016). XGBoost: a scalable tree boosting system. In Proceedings of the 22nd ACM SIGKDD International Conference on Knowledge Discovery and Data Mining (pp. 785-794).
18. Lundberg, S.M., Lee, S.-I. (2017). A unified approach to interpreting model predictions. Advances in Neural Information Processing Systems, 30.
19. IS 12269:2013. Ordinary Portland Cement, 53 Grade - Specification. Bureau of Indian Standards, New Delhi.
20. IS 456:2000. Plain and Reinforced Concrete - Code of Practice. Bureau of Indian Standards, New Delhi. [21] IS 516:1959. Method of Tests for Strength of Concrete. Bureau of Indian Standards, New Delhi.
21. IS 383:1970. Specification for Coarse and Fine Aggregates from Natural Sources for Concrete. Bureau of Indian Standards, New Delhi.